

High-Dispersion Spectroscopic Study of Solar Twins: HIP 56948, HIP 79672, and HIP 100963 *

Yoichi TAKEDA

National Astronomical Observatory, 2-21-1 Osawa, Mitaka, Tokyo 181-8588
takeda.yoichi@nao.ac.jp

and

Akito TAJITSU

Subaru Telescope, 650 North A'ohoku Place, Hilo, Hawaii 96720, U.S.A.
tajitsu@subaru.naoj.org

(Received 2008 December 2; accepted 2009 January 7)

Abstract

An intensive spectroscopic study was performed for three representative solar twins (HIP 56948, HIP 79672, and HIP 100963) as well as for the Sun (Moon; reference standard), with an intention of (1) quantitatively discussing the relative-to-Sun similarities based on the precisely established differential parameters and (2) investigating the reason causing the Li abundance differences despite their similarities. It was concluded that HIP 56948 most resembles the Sun in every respect including the Li abundance (though not perfectly similar) among the three and deserves the name of “closest-ever solar twin”, while HIP 79672 and HIP 100963 have somewhat higher effective temperature and appreciably higher surface Li composition. While there is an indication of Li being rotation-dependent because the projected rotation in HIP 56948 (and the Sun) is slightly lower than the other two, the rotational difference alone does not seem to be so large as to efficiently produce the marked change in Li. Rather, this may be more likely to be attributed (at least partly) to the slight difference in T_{eff} via some T_{eff} -sensitive Li-controlling mechanism. Since the abundance of beryllium was found to be essentially solar for all stars irrespective of Li, any physical process causing the Li diversity should work only on Li without affecting Be.

Key words: stars: abundances — stars: atmospheres — stars: individual (HIP 56948, HIP 79672, HIP 100963) — stars: rotation — stars: solar analog

1. Introduction

Can we find such a star that indiscernibly resembles our Sun in every respect? This “solar twin¹ survey”, an ever-attracting subject for stellar astronomers, has made significant progress since 1990s, thanks to the improvement in the precision of stellar parameter determinations.

Since Porto de Mello and da Silva (1997) reported the remarkable similarity of HIP 79672 (= 18 Sco = HR 6060 = HD 146233; $V = 5.50$) to the Sun, this star has maintained the status of best solar twin candidate almost for a decade (see also Soubiran & Triaud 2004). In the meantime, by using a numerical technique developed by Takeda (2005; hereinafter referred to as Paper I) for establishing the parameter differences between two similar stars with high precision, Takeda et al. (2007; hereinafter Paper

II) conducted a comprehensive study of solar analog stars and found that HIP 100963 (= HD 195934; $V = 7.09$) is an equally good (or even better) solar twin as HIP 79672.

Yet, there is one concern. While these HIP 79672 and HIP 100963 are certainly very similar to the Sun in terms of the stellar parameters and the general appearance of the spectra, one marked dissimilarity exists in a particular part of the spectrum: the strength of Li line at 6707.8 Å in these two stars is appreciably stronger compared to the solar case (cf. figure 3 in Soubiran & Triaud 2004 and figure A.2 in Paper II). This decisive difference in the surface Li abundance is actually “a fly in the ointment,” which makes us somewhat hesitate to regard them as “real” solar twins.

Interestingly, however, Meléndez and Ramírez (2007) recently reported that HIP 56948 (= HD 101364; $V = 8.70$) appears to be an ideal solar twin in the sense that it has essentially solar parameters and the low Li abundance similarly to the Sun. If this is confirmed, this star may deserve being called as a genuine solar twin. It would thus be worth carrying out an independent check analysis in order to ascertain whether HIP 56948 really resembles our Sun on every point including the Li abundance.

Another related subject of interest is the cause of such a difference in the Li abundance among these superficially very similar solar twins. It was concluded in Paper II

* Based on data collected at Subaru Telescope, which is operated by the National Astronomical Observatory of Japan. The electronic tables E1 and E2 will be available at the E-PASJ web site upon publication, while they are provisionally placed at the WWW site of (<http://optik2.mtk.nao.ac.jp/~takeda/solartwins/>).

¹ We use the term “solar twin” for those special solar-type stars which have particularly high similarity to the Sun with respect to spectra as well as stellar parameters. See Appendix A of Takeda et al. (2007) and the references therein for the literature concerning this theme.

based on the analysis of 118 solar-analog dwarfs around early-G type that the surface Li abundance is closely correlated with the macroscopic line-broadening parameter (comprising macroturbulence plus rotation); i.e., the surface Li tends to be higher (i.e., less depleted) as the line-width becomes broader (cf. figure 13 therein). Since the macroturbulence (due to the granular motion of stellar convection origin) is unlikely to differ much among similar solar-type stars, this observational fact suggests that the most decisive factor controlling the surface Li abundance is the stellar rotation or the angular momentum (i.e., faster rotation tends to suppress the envelope mixing and leads to less depletion of Li). Then, is the distinction between the Li-strong (HIP 79672 and HIP 100963) and Li-weak (HIP 56948 and naturally the Sun itself) solar twins simply caused by the difference in the rotational velocity? This point should be checked by careful determinations of the projected rotational velocities of these stars.

Besides, we should also pay attention to two other related viewpoints in connection with this “rotation–mixing–surface Li” relationship. The first is the stellar activity which tends to diminish/enhance as the rotation becomes slower/faster. If the rotation is the key factor affecting the surface Li, does the Li-strong solar twins show higher activity than Li-weak ones? The second is the surface abundance of beryllium, which is destroyed when conveyed into the hot stellar interior by envelope mixing similarly to lithium at temperature of $T \sim 3.5 \times 10^6$ K (higher than the case of Li which is burned at $T \sim 2.5 \times 10^6$ K). It is interesting to see whether any difference is observed in the surface abundance of Be between the Li-strong and Li-weak groups, which may provide us with an observational constraint on the origin of Li discrepancies among these solar twins

Motivated by these considerations, we decided to conduct an intensive spectroscopic study for these representative solar twins (HIP 56948, HIP 79672, and HIP 100963 along with the Sun/Moon as the comparison standard) based on the high-dispersion spectra obtained by the Subaru Telescope with HDS, in order to (1) quantitatively discuss the relative-to-Sun similarities of these three stars while precisely establishing their “star–Sun” differential parameters by applying the method of Paper I and to (2) investigate the reason/mechanism causing the difference between the Li-strong and Li-weak groups by examining the rotational velocity, the degree of stellar activity, and the Li as well as Be abundance. This is the purpose of this study.

2. Observational Data

The observations of HIP 56948, HIP 79672, HIP 100963 and the Moon (substitute for the Sun) were carried out in the night of 2008 June 15 (Hawaii Standard Time) by using the High Dispersion Spectrograph (HDS; Noguchi et al. 2002) placed at the Nasmyth platform of the 8.2-m Subaru Telescope, which can record high-dispersion spectra covering a wavelength portion of $\sim 1600\text{\AA}$ (blue cross

disperser) or $\sim 2600\text{\AA}$ (red cross disperser) with two CCDs of $2K \times 4K$ pixels at a time.

In order to cover the wide wavelength range from near-UV ($\sim 3000\text{\AA}$) to red ($\sim 7000\text{\AA}$), each star was observed at two different wavelength settings (standard Ub with blue cross disperser for $\sim 3000\text{--}4500\text{\AA}$ and standard Yc with red cross disperser for $\sim 4400\text{--}7000\text{\AA}$). With the slit width set at $0.''4$ ($200\text{ }\mu\text{m}$) and no on-chip binning of pixels, the resolving power of the obtained spectra is $R \simeq 90000$. The integrated exposure times for each star at Ub/Yc settings are 64 min/32 min, 18 min/7 min, 32 min/16 min, and 2 min/0.5 min for HIP 56948, HIP 79672, HIP 100963 and the Moon, respectively.

The reduction of the spectra (bias subtraction, flat-fielding, scattered-light subtraction, spectrum extraction, wavelength calibration, continuum normalization) was performed by using the “echelle” package of the software IRAF² in a standard manner. The estimated S/N ratios at each of the wavelengths calculated as the square root of the resulting photoelectron counts ($\text{ADN} \times \text{gain}$) are graphically depicted in figure 1. We can see from this figure that sufficiently high S/N ratios of $\sim 500\text{--}1000$ are achieved in the most sensitive red region, though this value is considerably reduced even by a factor of ~ 10 at $\sim 3100\text{\AA}$ of near-UV where Be II lines are located.

3. Parameter Determination

3.1. Standard Stellar Parameters

Following the procedure described in subsection 3.1.1 of Paper II, we measured the equivalent widths (EW) of Fe I and Fe II lines on the “Yc setting” spectra covering $\sim 4400\text{--}7000\text{\AA}$. Based on these EW values, the four standard³ atmospheric parameters [$T_{\text{eff}}^{\text{std}}$ (effective temperature), $\log g$ (surface gravity), v_t (microturbulent velocity dispersion), and $\{\text{Fe}/\text{H}\}^{\text{std}} [\equiv A_{\text{Fe}}^{\text{std}} - 7.50]$ (Fe abundance⁴)], which are necessary for constructing model atmospheres, were spectroscopically derived by using the TGVIT program (Takeda et al. 2005; cf. section 2 therein). This method is based on the principle searching for the most optimum solution in the 3-dimensional (T_{eff} , $\log g$, v_t) space such that simultaneously satisfying the three requirements of (i) the excitation equilibrium, (ii) the ionization equilibrium, and (iii) the EW-independence of the abundances (cf. Takeda, Ohkubo, & Sadakane 2002). The detailed EW data and the Fe abun-

² IRAF is distributed by the National Optical Astronomy Observatories, which is operated by the Association of Universities for Research in Astronomy, Inc. under cooperative agreement with the National Science Foundation.

³ We use the notation of “standard” here, which means that these have characters of “absolute” parameters in the usual sense, in order to discriminate them from the “differential” parameters (relative to the Sun) presented in subsection 3.5.

⁴ We intentionally expressed this quantity as $\{\text{Fe}/\text{H}\}$, in order to clarify that it is still an absolute quantity (i.e., essentially equivalent to $A_{\text{Fe}}^{\text{std}}$) and should be distinguished from the strictly differential metallicity relative to the Sun, $[\text{Fe}/\text{H}] (\equiv A_{\text{Fe}}^{\text{star}} - A_{\text{Fe}}^{\text{sun}})$, which is also denoted as ΔA_{Fe} in subsection 3.5.

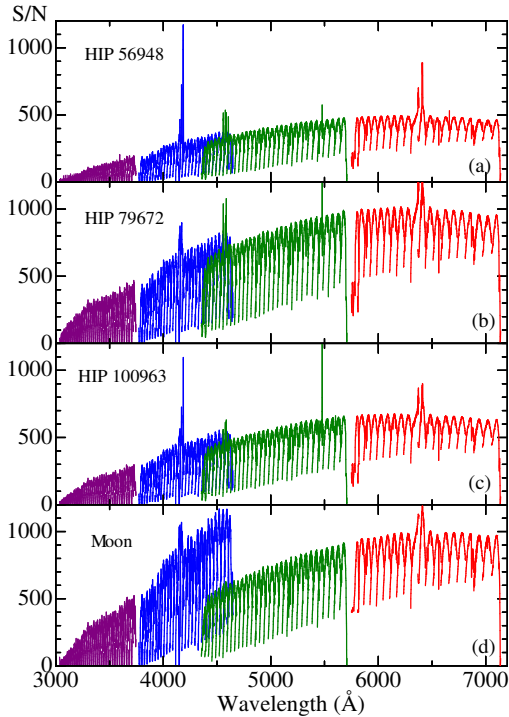


Fig. 1. Distribution of S/N ratios (estimated as the square root of photoelectron counts) of the spectra used for this study, which are divided into four wavelength regions: $\sim 3000\text{--}3700$ Å (blue CCD) and $\sim 3700\text{--}4600$ Å (red CCD) in the Ub setting; $\sim 4400\text{--}5700$ Å (blue CCD) and $\sim 5700\text{--}7000$ Å (red CCD) in the Yc setting. The absence of data at ~ 3700 Å and ~ 5700 Å corresponds to the joint of mosaicked CCDs. Spurious spikes seen at several wavelengths are due to bad columns of CCDs. (a) HIP 56948, (b) HIP 79672, (c) HIP 100963, and (d) Moon.

dances corresponding to the final parameters for each star are presented in electronic table E1. The results are summarized in table 1, where the related stellar parameters (L , M , and age) evaluated as in subsection 3.3 of Paper II are also given.

Comparing the present EW data measured from the Subaru/HDS spectra ($R \simeq 90000$, S/N $\sim 500\text{--}1000$) with those from OAO/HIDES spectra in Paper II and Paper I ($R \simeq 70000$, S/N $\sim 200\text{--}600$), we confirmed a general consistency as shown in figure 2. However, a close inspection revealed a slight systematic difference in the sense that EW(Subaru) tends to be by $\sim 1\text{--}2\%$ smaller than EW(OAO). According to this delicate systematic change, marginal differences are seen in the present results of such absolute parameters when compared to those in these previous papers; e.g., for the case of the Sun/Moon, T_{eff} and $\{\text{Fe}/\text{H}\}$ have been lowered by ~ 30 K and ~ 0.03 dex, respectively, though these changes should not matter in the differential analysis (subsection 3.5).

3.2. Rotational Velocity

In order to evaluate the stellar projected rotational velocity ($v_e \sin i$), we determined the total macrobroadening parameter, v_M , which is the e -folding width

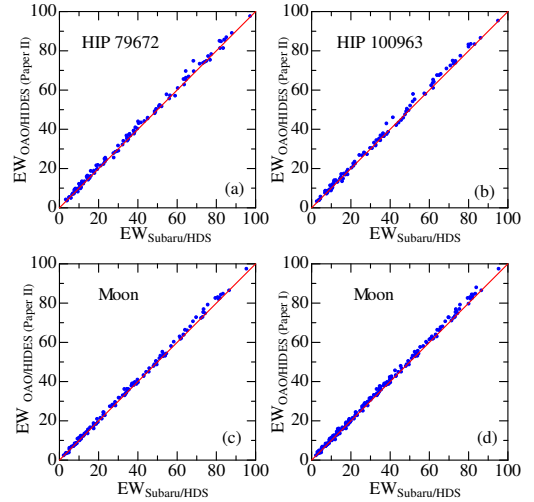


Fig. 2. Comparison of the equivalent widths of Fe I and Fe II lines measured on the Subaru/HDS spectra for the determinations of atmospheric parameters in this study (abscissa) with those used in the previous investigations based on the OAO/HIDES spectra (ordinate). (a) HIP 79672 (Paper II), (b) HIP 100963 (Paper II), (c) Moon (Paper II), and (d) Moon (Paper I).

of the Gaussian macrobroadening function, $f_M(v) \propto \exp[-(v/v_M)^2]$, by way of the line-profile fitting as done in subsection 4.2 of Paper II. Unlike the previous case (where the fitting was applied to the spectrum portion at the $6080\text{--}6089$ Å region), however, we performed the fitting analysis to each of the “individual” Fe I and Fe II lines (the same lines as used for the EW measurements in subsection 3.1) as Takeda (1995) did for the solar flux spectrum, because the macroturbulence (to be subtracted from the total macrobroadening) is considered to be different from line to line because of its depth-dependence (cf. Takeda 1995).

We used the line-broadening model adopted by Takeda et al. (2008). That is, the total macrobroadening function, $f_M(v)$, is assumed to be the convolution of three Gaussian component functions $f_\alpha \propto \exp[-(v/v_\alpha)^2]$, where α is any of “ip” (instrumental profile), “rt” (rotation), and “mt” (macroturbulence); i.e.,

$$v_M^2 = v_{\text{ip}}^2 + v_{\text{rt}}^2 + v_{\text{mt}}^2 \quad (= v_{\text{ip}}^2 + v_{\text{r+m}}^2), \quad (1)$$

where $v_{\text{r+m}}$ is the “macroturbulence+rotation” parameter used in Paper II. These broadening parameters (v_{ip} , v_{rt} , and v_{mt}) may be related to the more realistic quantities as $v_{\text{ip}} \simeq (c/R)/(2\sqrt{\ln 2})$ (2.00 km s $^{-1}$ in the present case of $R \simeq 90000$), $v_{\text{rt}} \simeq 0.94v_e \sin i$ (v_e and i are the equatorial rotation velocity and the inclination angle), and $v_{\text{mt}} \simeq 0.42\zeta_{\text{RT}}$ (ζ_{RT} : radial-tangential macroturbulence dispersion; cf. Gray 2005), as explained in footnotes 10 and 12 of Takeda et al. (2008).

Further, since we may reasonably postulate that the macroturbulence velocity field in the solar atmosphere can be applied to all of the three solar twin targets, we assume an analytical form of the depth-dependent macroturbu-

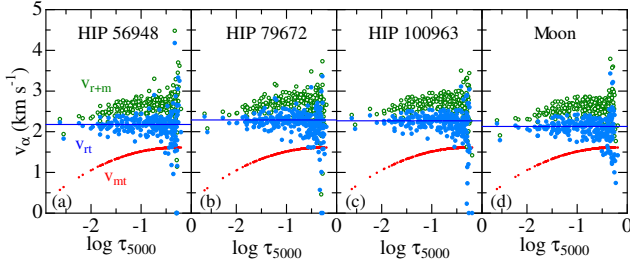


Fig. 3. Line-broadening parameters (derived by the profile-fitting method applied to blend-free Fe lines) plotted against the mean-depth of line formation ($\langle \log \tau_{5000} \rangle$), where green open circles, blue filled circles, and red dots represent v_{r+m} (rotation+macroturbulence), v_{mt} (macroturbulent velocity parameter, supposed to be depth-dependent as $v_{mt} = 1.60 - 0.11 \log \tau_{5000} - 0.19 \log \tau_{5000}^2$; cf. subsection 3.2) and v_{rt} (rotational broadening parameter obtained as $(v_{r+m}^2 - v_{mt}^2)^{1/2}$), respectively. The blue horizontal line indicates the average value of v_{rt} ($\langle v_{rt} \rangle$; cf. table 1) calculated for the lines of $\langle \log \tau_{5000} \rangle \leq -0.7$. (a) HIP 56948, (b) HIP 79672, (c) HIP 100963, and (d) Moon.

lence (in terms of τ_{5000} , the optical depth at 5000 Å)

$$v_{mt} (= 0.42 \zeta_{RT}) = 1.60 - 0.11 \log \tau_{5000} - 0.19 \log \tau_{5000}^2, \quad (2)$$

since ζ_{RT} may be approximately expressed as $3.8 - 0.25 \log \tau_{5000} - 0.45 \log \tau_{5000}^2$ from figure 2 of Takeda (1995).

Now the procedure makes as follows.

- (1) First, v_M is determined by applying the profile-fitting method to a blend free Fe line.
- (2) Then, v_{r+m} (macroturbulence plus rotation) is obtained by subtracting the instrumental broadening effect ($v_{ip} = 2.00 \text{ km s}^{-1}$) as $v_{r+m} = \sqrt{v_M^2 - v_{ip}^2}$.
- (3) From the measured equivalent width, the mean-depth of line formation ($\langle \log \tau_{5000} \rangle$) relevant for this line can be computed (cf. subsection 5.1 in Takeda 1995), which is sufficient to assign an appropriate value of v_{mt} to this line with the help of equation (2).
- (4) Eventually, v_{rt} is evaluated as $v_{rt} = \sqrt{v_{r+m}^2 - v_{mt}^2}$.

While the detailed results of v_{r+m} and v_{rt} (along with the assigned $\langle \log \tau_{5000} \rangle$) for each line are presented in electronic table E2, these v_{r+m} , v_{mt} , and v_{rt} are plotted against τ_{5000} in figure 3. We can see from this figure that the depth-dependent tendency of v_{r+m} is almost removed in v_{rt} by subtracting the effect of v_{mt} . Finally, we obtained $\langle v_{rt} \rangle$ as the parameter representing $v_e \sin i^5$ by averaging the v_{rt} 's with $\langle \log \tau_{5000} \rangle \leq -0.7$ (deep-forming lines with

⁵ Admittedly, we can not hope to relate the “exact” value of $v_e \sin i$ to $\langle v_{rt} \rangle$ within the framework of such a rough modeling of line-broadening functions (all assumed to be the Gaussian form). However, we may reasonably expect that $\langle v_{rt} \rangle$ is proportional to $v_e \sin i$ with a factor not much different from unity. This is sufficient for our present purpose, because what we want to know is the “differential” characteristics (i.e., the ratio of $\langle v_{rt} \rangle$ between two stars is considered to be the ratio of actual $v_e \sin i$). At any rate, it is encouraging that the resulting $\langle v_{rt} \rangle$ value of 2.13 km s^{-1} for the Sun/Moon is quite close to the actual solar $v_e \sin i$ value of 1.9 km s^{-1} , by which we may regard that our approximation (suggesting $v_{rt} \simeq 0.94 v_e \sin i$) is not bad.

$\langle \log \tau_{5000} \rangle \geq -0.7$ were not used for the averaging because of the larger uncertainties due to the weakness of the line-strength), as given in table 1.

3.3. Li Abundance

The portion of the observed spectrum (6706.3–6709.3 Å) comprising the Li I resonance doublet at $\sim 6707.8 \text{ Å}$, along with Kurucz et al.’s (1984) solar flux spectrum, is shown in figure 4 (left panels). We can recognize from this figure that the strengths of the Li line for HIP 79672 and HIP 100963 are markedly larger than those for HIP 56948 and the Sun/Moon, classifying these four into Li-strong and Li-weak groups. As in Paper II, the Li abundance (A_{Li}) was determined from the Li I doublet lines at $\sim 6707.8 \text{ Å}$ in the same manner as described in Takeda and Kawanomoto (2005). Namely, we first establish the LTE abundance ($A_{\text{Li}}^{\text{LTE}}$) by applying the method of synthetic profile fitting to the spectrum feature of Fe I + Li I lines (see the right panels in figure 4). Then, the EW(Li I 6708) is inversely calculated from such obtained $A_{\text{Li}}^{\text{LTE}}$. Finally, while taking into account the non-LTE effect, $A_{\text{Li}}^{\text{NLTE}}$ is calculated from EW(Li I 6708). The resulting $A_{\text{Li}}^{\text{LTE}}$ for each star is presented in table 1. In all the four cases studied, the non-LTE correction $\Delta (\equiv A_{\text{Li}}^{\text{NLTE}} - A_{\text{Li}}^{\text{LTE}})$ turned out to be +0.07. The solar Li abundance of 0.91 derived in this study based on the spectrum of Moon (Subaru/HDS) is in excellent agreement with the result of 0.92 concluded by Takeda and Kawanomoto (2005) based on the spectrum of Moon (OAO/HIDES) as well as the solar flux spectrum (Kurucz et al. 1984).

3.4. Be Abundance

The spectrum portion of 3129.5–3131.5 Å comprising Be II lines at 3130.42 Å and 3131.07 Å is shown in figure 5, where each stellar spectrum is compared with Kurucz et al.’s (1984) solar flux spectrum. A glance of this figure suffices us to convince that Be line features are essentially the same as the solar case for all stars. According to the theoretical simulation shown in the lowest panel of this figure, the agreement of A_{Be} with the solar value appears to be very good, presumably to within ~ 0.1 dex (though the uncertainty may be somewhat larger for HIP 56948 where the spectrum quality is comparatively poor). This fact clearly suggests that Be makes a clear distinction from Li (showing an appreciable difference from star to star) in spite of their rather similar characters comparatively easily destroyed in the stellar interior, at least for these solar twin stars are concerned. This result is consistent with what Randich et al. (2002) concluded for early-G dwarf stars in open clusters.

3.5. Differential Analysis

Now that the “standard” atmospheric parameters were established in subsection 3.1, we can derive the “differential” parameters Δp_{i-j} (p is any of T_{eff} , $\log g$, v_t , and A_{Fe}) of star i relative to any other arbitrary comparison star j by using the method described in Paper I, where several practical quantities were defined such as (i) the

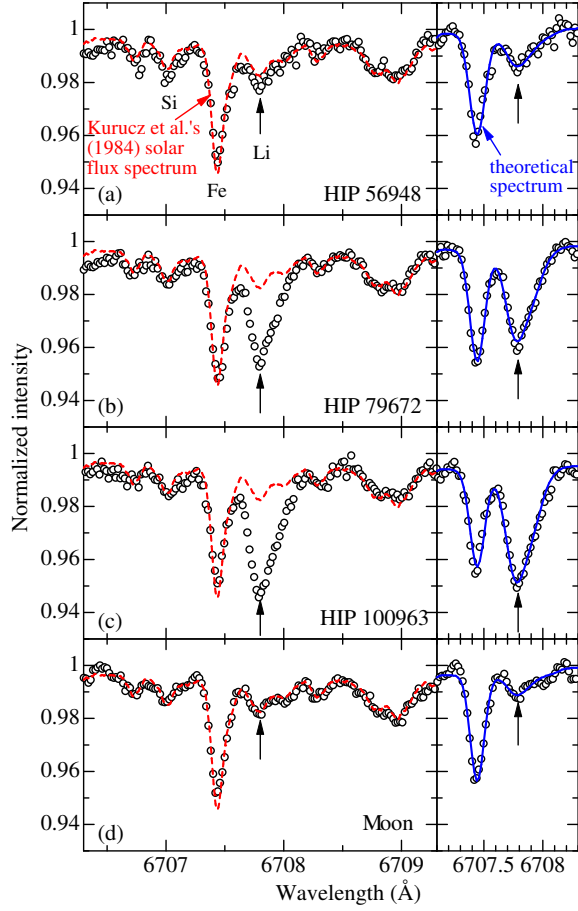


Fig. 4. Left side: Observed spectra of target stars in the spectrum region comprising Li I 6707.8 line (open symbols) in comparison with the solar flux spectrum (red dashed line). Right side: Theoretically simulated spectrum in the Li I 6707.8 line region (blue solid line) fitted with the observed stellar spectrum (open symbols). (a) HIP 56948, (b) HIP 79672, (c) HIP 100963, and (d) Moon.

average of the direct solution, $\langle \Delta p_{ij} \rangle$ (average of Δp_{i-j} and $-\Delta p_{j-i}$), (ii) the intermediary solution via star k , $\langle \Delta p_{i(k)j} \rangle$ ($\equiv \langle \Delta p_{ik} \rangle + \langle \Delta p_{ik} \rangle$), and (iii) the average of the intermediary solution, $\langle \langle \Delta p_{i(j)} \rangle \rangle$ (average of $\langle \Delta p_{i(k)j} \rangle$ over various k).

Since we are interested in the parameter differences relative to the Sun, we take $i = 1, 2, 3$ and $j = 0$ (see table 1 for the numbering of each star), and two intermediary stars can be assigned for any pair (e.g., for the case of $i = 1$ and $j = 0$, we can take $k = 2$ or $k = 3$). The detailed results for HIP 56948 ($i = 1$), HIP 79672 ($i = 2$), HIP 100963 ($i = 3$) are presented in tables 2, 3, and 4, respectively. (Note that these three tables are formatted in the same manner as in tables 2–9 of Paper I.) The values of $\langle \Delta p_{i0} \rangle$ (direct solution) and $\langle \langle \Delta p_{i(j)0} \rangle \rangle$ (average of the intermediary solution) are separately summarized in table 5, where the differences in v_{rt} and A_{Li} are also given. It is worth noting that the comparison of these two direct and intermediary solutions may provide us with an opportunity of

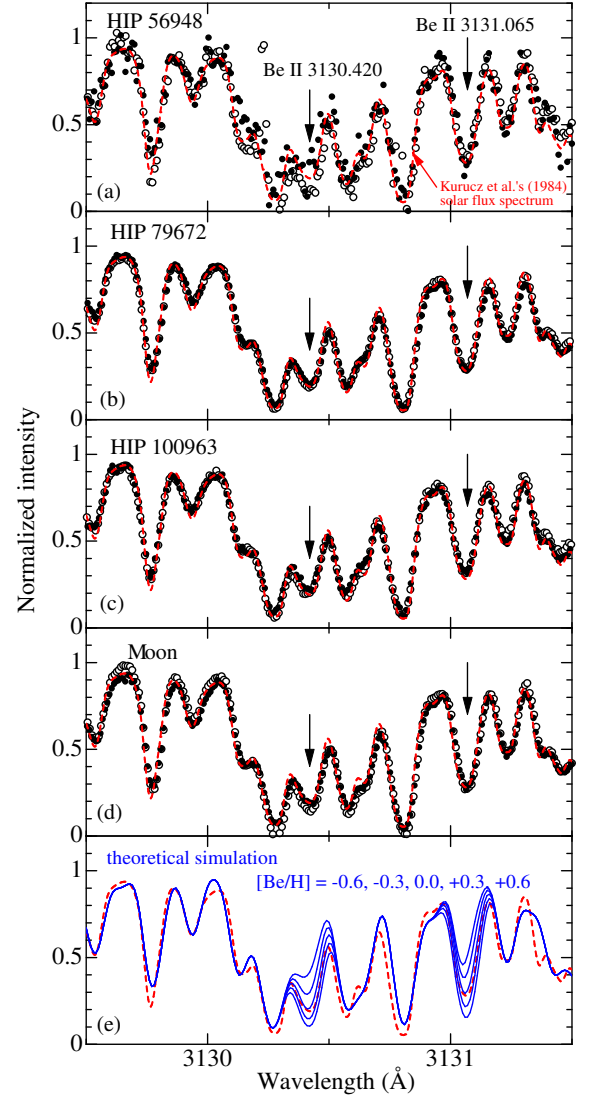


Fig. 5. Observed spectra of target stars in the near UV region comprising two Be II lines at 3130.42 and 3130.07 Å (symbols: filled and open circles correspond the spectra of different echelle orders 189 and 190, respectively), in comparison with Kurucz et al.'s (1984) solar flux spectrum (red dashed line). The continuum level of each spectrum has been so adjusted as to achieve a consistency between the stellar and the reference solar spectrum. (a) HIP 56948, (b) HIP 79672, (c) HIP 100963, and (d) Moon. In the lowest panel (e), theoretically synthesized spectra for Sun (blue solid lines), are compared with the solar flux spectrum (red dashed line), which were computed by using the atomic data given in Primas et al. (1997) with different Be abundances of $[\text{Be}/\text{H}] = -0.6, -0.3, 0.0, +0.3, \text{ and } +0.6$.

checking/estimating the accuracy of the results.

4. Discussion

4.1. Which Is the Best Solar Twin?

When we compare the parameter differences (relative to the Sun) for HIP 79672 and HIP 100963 given in table 5 with those of Paper II (see table A.1 therein), we see a notable discrepancy in the values of ΔT_{eff} , despite that other $\Delta \log g$, Δv_t , and ΔA_{Fe} are mostly in good agreement. Namely, while Paper II derived very small ΔT_{eff} (+1.7 K/−1.6 K for HIP 79672/100963), the present results (+48.5 K/+38.2 K for the direct solution) indicate appreciably larger values by ~ 40 –50 K than these. Although the reason for this ΔT_{eff} discrepancy is not clear, it would presumably be ascribed to the difference in the used EW data set. At any rate, because of the reasonable consistency between the direct and intermediary solutions (compare the values in the upper and lower rows in table 5) and the use of the spectrum data of much higher quality (in terms of both the S/N ratio and the spectrum resolving power), we would place larger weight in the present results.

By inspecting table 5, we can summarize as follows concerning the similarity or dissimilarity of these three program stars to the Sun in terms of each checkpoint. (In the discussion of the parameter differences given below, we refer to the averaged values of the direct and intermediary solutions for convenience.)

- ΔT_{eff} : HIP 56948 is manifestly more solar like ($\sim +10 \pm 10$ K) than other HIP 79672 and HIP 100963 ($\sim +40 \pm 10$ K).
- $\Delta \log g$: All three stars do not show appreciable differences from the solar value, if we consider the nominal uncertainty of ~ 0.01 dex.
- Δv_t : HIP 79672 shows slightly higher v_t than the Sun by $+0.03$ – 0.04 km s $^{-1}$, HIP 56948 and HIP 100963 are essentially solar.
- ΔA_{Fe} : Regarding the metallicity, HIP 100963 is almost indiscernible from the Sun ($\lesssim 0.01$ dex) and HIP 56948 ($\sim +0.01$ – 0.02 dex) is also near-solar (or very slightly metal-rich?), while HIP 79672 appears to be somewhat metal-rich ($\sim +0.05$ dex).
- A_{Li} : HIP 79672 and HIP 100963 are markedly overabundant in Li compared to the Sun by $\sim +0.7$ – 0.8 dex (by a factor of ~ 5 – 6), while the difference from $A_{\text{Li},\odot}$ is much milder for HIP 56946 (only $\sim +0.2$ dex or $\sim 60\%$).
- $\langle v_{\text{rt}} \rangle$ (equivalent to $v_e \sin i$): HIP 56948 has almost the same projected rotational velocity as the Sun, while HIP 79672 and HIP 100963 show slightly higher values by ~ 5 – 10% .
- A_{Be} : All three stars (HIP 56948, HIP 79672, and HIP 100963) have essentially the same Be abundances as the Sun, which means that Be does not conform to the behavior of Li showing a diversity. Consequently, whichever mechanism changing the surface Li abundance of these solar twins can not

influence Be; e.g., if the variation of A_{Li} is caused by an envelope mixing, it should not be so deep as to affect Be (see also Randich et al. 2002).

Taking all these results into consideration, we can draw the following conclusions.

HIP 56948 is surely most similar to the Sun among these three stars, not only from the similarity of stellar parameters but also from the viewpoint of surface Li abundance; it may thus deserve the name of “closest ever solar twin.” However, unlike the argument of Meléndez and Ramírez (2007) who derived $\Delta A_{\text{Li}} = -0.02(\pm 0.13)$, since the atmospheric Li abundance of this star is marginally higher than the solar value by ~ 0.2 dex, we still can not call it a “genuine” solar twin. Another concern about this star is that its luminosity derived from the Hipparcos parallax appears to somewhat larger than the solar luminosity, which in effect makes the age older (cf. table 1). We suspect that this inconsistency is attributed to the error in the parallax because HIP 56948 is comparatively distant. The possibility that its actual π is by $\sim 10\%$ larger than the catalogued value may as well be considered, since the similarity of T_{eff} , $\log g$, and A_{Fe} should guarantee the equality of L (cf. Appendix A of Paper II).

Regarding HIP 79672 and HIP 100963, they have by ~ 40 K higher T_{eff} than $T_{\text{eff},\odot}$, by ~ 0.7 – 0.8 dex larger A_{Li} than $A_{\text{Li},\odot}$, and by ~ 5 – 10% larger $v_e \sin i$ than $v_e \sin i_{\odot}$. Apart from these considerable differences, the parameters of HIP 100963 quite resemble the solar values. Meanwhile, HIP 56948 shows other noticeable differences from the Sun with respect to v_t (by $+0.03$ – 0.04 km s $^{-1}$) and A_{Fe} ($\sim +0.05$ dex), which makes this star comparatively lower ranked as a solar twin among the three.

4.2. What Controls Lithium? — Roles of Rotation and T_{eff}

Let us turn our attention to the question posed in section 1: “why these solar twins show a diversity in the Li line strength in spite of their similarity to one another?” Is this attributed to the difference in the rotational velocity, as suggested in Paper II? According to tables 1 and 5, the values of $v_{\text{rt}} (\simeq v_e \sin i)$ for the Li-strong group (HIP 79672 and HIP 100963) are somewhat larger by ~ 5 – 10% than those for the Li-weak group (HIP 56948 and the Sun/Moon), which can also be visually recognized in figure 3. Considering that $i = 90^\circ$ for the Sun while i is unknown for the three stars, we can assure that the equatorial rotational velocities (v_e) of Li-strong HIP 79672 and HIP 100963 are anyhow larger than the solar value ($v_{e,\odot}$), which may be just favorable for the working hypothesis of Paper II.

Yet, we feel it still premature to conclude that the stellar rotation is the only decisive factor to influence the surface Li abundance of these solar twin stars. Inspecting the core features of Ca II H and K lines of the program stars shown in figure 6, which are sensitive to the chromospheric activity closely related to the stellar rotation rate,⁶ we see in any of these stars almost no apprecia-

⁶ The strength of the Ca II H+K core emission is known to roughly

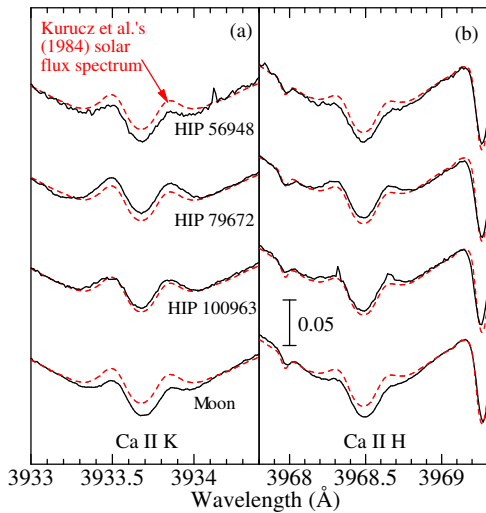


Fig. 6. Emission features in (a) Ca II K and (b) Ca II H resonance line cores of the program stars (solid lines), compared with Kurucz et al.’s (1984) solar flux spectrum (red dashed line). The continuum level of each spectrum (with a vertical offset of 1.0 relative to the adjacent one) has been appropriately adjusted so that the stellar spectrum matches the reference solar spectrum at $\Delta\lambda \sim \pm 0.5\text{\AA}$. (a) HIP 56948, (b) HIP 79672, (c) HIP 100963, and (d) Moon.

ble differences in comparison to the solar H and K cores of Kurucz et al.’s (1984) solar spectrum. (Actually, the largest difference relative to the Sun among the four is seen in the “Moon” spectrum, which is presumably due to the difference in the solar activity phase, because the year of 2008 corresponds to the almost minimum activity.) Besides, according to Giampapa (2005; cf. figure 36 therein), the Li-strong HIP 79672 exhibits the stellar activity (inferred from Ca II H and K line cores; amplitude of $\sim 10\%$ with period of 8–9 years) quite similar to the solar activity. We thus consider that “substantially” large difference in the rotational rate is not very likely between Li-strong (HIP 79672 and HIP 100963) and Li-weak (HIP 56948 and the Sun) groups.

We rather suspect that the difference in T_{eff} may also play a significant role in producing this Li-diversity. As reported in Paper II, there is a slanted “lower boundary line” at $+100\text{ K} \gtrsim \Delta T_{\text{eff}} \gtrsim 0\text{ K}$ in the A_{Li} vs. ΔT_{eff} diagram, below which no stars are found (cf. figure 9 therein). Interestingly, when we plot HIP 79672 and HIP 100963 (both have $\Delta T_{\text{eff}} \sim +50\text{ K}$ and $A_{\text{Li}} \sim 1.6$) on this diagram, they almost fall on this boundary line, $A_{\text{Li}} \simeq 1 + 1(\Delta T_{\text{eff}}/100\text{K})$, which we regard to be a significant fact being worth attention.

That is, as speculated in Paper II, we consider that the diversity of A_{Li} (at a given T_{eff}) is due to the difference in the rotational velocity (i.e., slower rotators tend to show

lower Li abundances presumably caused by an enhanced envelope-mixing). On the other hand, since the existence of steeply-slanted lower boundary of A_{Li} means that every slow rotators should settle on this boundary line, the A_{Li} values of such slow rotators would naturally show the marked T_{eff} -dependence of $dA_{\text{Li}}/d(T_{\text{eff}}/100\text{K}) \sim 1$. This scenario may reasonably explain (at least to an order of magnitude) the difference in A_{Li} by ~ 0.6 – 0.7 dex between HIP 79672/HIP 100963 and Sun/HIP 79672, all showing superficially slow rotation as the Sun, while T_{eff} for the former being slightly higher than the latter by ~ 40 – 50 K . Consequently, the Li-strong nature of HIP 79672 and HIP 100963 may be naturally explained by the fact that they belong to the “boundary-line stars” (which seem to have higher possibilities of hosting planets; cf. subsection 5.1 in Paper II). In this sense, we would suggest that T_{eff} is another significant factor (along with rotational velocity v_e) in controlling the lithium abundances of solar twins, especially for slowly-rotating ones.

Anyway, this is nothing but a phenomenological explanation, and a number of tasks are still left until the real physical mechanism involved in determining the surface Li abundance is clarified. Hence, investigations (especially on the theoretical side) on the inter-relations between rotation, T_{eff} , and A_{Li} in solar-analog stars are desirably awaited, so that the confronted problems could be settled:

- Why does such a slanted lower boundary exist in the A_{Li} vs. T_{eff} diagram of solar-analog stars, below which stars do not exist (“forbidden zone”)? Any T_{eff} -sensitive physical mechanism is acting so as to suppress the further Li depletion?

- A_{Li} appears to be positively correlated with both $v_e \sin i$ and T_{eff} . What does this mean? These two factors happen to act independently on A_{Li} in the same direction? Or this is nothing but a superficial effect caused by a tight relationship between $v_e \sin i$ and T_{eff} ?

- Whichever $v_e \sin i$ or T_{eff} may be the relevant key, the physical mechanism working in the envelope of these solar analog stars must satisfy the condition of changing the surface Li without affecting Be. What kind of process is that?

- Finally, from the observational side, the number of well-studied solar twins/analogs is still so insufficient as to clearly reveal the behavior of Li in Sun-like stars. If we could considerably increase the number of the sample stars (e.g., $\sim 10^3$ or even more), it would surely give us a new insight to this field (in addition, a nearly-perfect solar twin might as well be detected). Besides, given that field solar-type stars are diverse in their age (cf. figure 10 in Paper II), intensively studying the early-G dwarfs in old solar-age clusters (e.g., M 67) would also be beneficial for disentangling the roles of various stellar parameters on this Li problem.

5. Conclusion

An intensive spectroscopic study based on the high-quality spectra obtained with Subaru/HDS was performed

scale with the rotational rate (e.g., Noyes et al. 1984), though its exact relationship is still under discussion (see, e.g., Giampapa 2005). This means, for example, that a solar-type star rotating with $v_e \sim 10\text{ km s}^{-1}$ would show a stronger core emission by several times than the Sun.

for HIP 56948, HIP 79672, and HIP 100963 (along with the Sun/Moon as the reference standard), known to be the representative solar twins, in order to (1) clarify which of the three most resembles the Sun by precisely establishing the various differential parameters relative to the Sun and (2) investigate the reason why appreciable differences in the surface Li abundance are observed for these superficially very similar stars.

The standard atmospheric parameters ($T_{\text{eff}}^{\text{std}}$, $\log g^{\text{std}}$, $v_{\text{t}}^{\text{std}}$, and $\{\text{Fe}/\text{H}\}^{\text{std}}$) were first evaluated by using the equivalent widths of Fe I and Fe II lines, the rotational velocity parameter (v_{rt} ; which is nearly equivalent to $v_{\text{e}} \sin i$) was derived from the line-profile width by eliminating the effect of the macroturbulence, and the lithium abundance (A_{Li}) was determined from the Li I doublet line at $\sim 6707.8 \text{ \AA}$. Further, the differences of atmospheric parameters (ΔT_{eff} , $\Delta \log g$, Δv_{t} , and ΔA_{Fe}) relative to the Sun were established by using the method of precision differential analysis (Paper I).

While we could confirm that HIP 79672/100963 have appreciably higher Li content by a factor of $\sim 5\text{--}6$ as compared to Sun/HIP 56948, the Be abundances for all the program stars (HIP 56948/79672/100963) turned out to be essentially the same as the solar value, which indicates that Be is not affected by any mechanism causing the variation of Li.

We found that HIP 56948 is most similar to the Sun among the three, not only from the similarity of stellar parameters (including rotation) but also from the weakness of the Li line (however, A_{Li} for this star is still slightly larger than $A_{\text{Li},\odot}$ by ~ 0.2 dex; i.e., not perfectly the same). It may thus deserve the name of “closest ever solar twin.” Meanwhile, some remarkable differences from the solar parameters are recognized in HIP 79672 and HIP 100963, which show somewhat higher T_{eff} (by ~ 40 K) considerably larger A_{Li} (by $\sim 0.7\text{--}0.8$ dex) and slightly higher rotational velocity (by $\sim 5\text{--}10\%$).

We can see a tendency that the Li-strong HIP 79672 and HIP 100963 have somewhat larger rotational velocity by $\sim 5\text{--}10\%$ than Li-weak HIP 56948 and the Sun, which is consistent with the suggestion of Paper II that A_{Li} is closely correlated with the stellar rotational velocity. However, it does not seem very likely that a substantial difference exists in the rotational velocity between these two groups, because no essential differences are seen in their chromospheric activities (sensitive to stellar rotation) inferred from Ca II H+K line cores. We rather suspect that the overabundance of Li in HIP 79672 and HIP 100963 (by $\sim 0.6\text{--}0.7$ dex) is attributed to the difference in T_{eff} (by $\sim +50$ K) relative to the Sun, since these two stars fall on the T_{eff} -sensitive slanted lower boundary in the A_{Li} vs. T_{eff} distribution as reported in Paper II for solar analog stars. However, it is not clear whether and how these two factors (rotational velocity and effective temperature) are mutually related in affecting the surface Li abundance, which remains to be further clarified.

References

- ESA 1997, The Hipparcos and Tycho Catalogues, ESA SP-1200, available from NASA-ADC or CDS in a machine-readable form (file name: `hip_main.dat`)
- Giampapa, M. 2005, in The Sun, Solar Analogs, and the Climate, Saas-Fee Advances Course 34/2004, (Berlin: Springer), p.307
- Gray, D. F. 2005, The Observation and Analysis of Stellar Photospheres, 3rd ed. (Cambridge: Cambridge University Press)
- Kurucz, R. L., Furenlid, I., Brault, J., & Testerman, L. 1984, Solar Flux Atlas from 296 to 1300 nm (Sunspot, New Mexico: National Solar Observatory)
- Meléndez, J., & Ramírez, I. 2007, ApJ, 669, L89
- Noyes, R. W., Hartmann, L. W., Baliunas, S. L., Duncan, D. K., & Vaughan, A. H. 1984, ApJ, 279, 763
- Noguchi, K., et al. 2002, PASJ, 54, 855
- Porto de Mello, G. F., & da Silva, L. 1997, ApJ, 482, L89
- Primas, F., Duncan, D. K., Pinsonneault, M. H., Deliyannis, C. P., & Thorburn, J. A. 1997, ApJ, 480, 784
- Randich, S., Primas, F., Pasquini, L., & Pallavicini, R. 2002, A&A, 387, 222
- Soubiran, C., & Triaud, A. 2004, A&A, 418, 1089
- Takeda, Y. 1995, PASJ, 47, 337
- Takeda, Y. 2005, PASJ, 57, 83 (Paper I)
- Takeda, Y., & Kawanomoto, S. 2005, PASJ, 57, 45
- Takeda, Y., Kawanomoto, S., Honda, S., Ando, H., & Sakurai, T. 2007, A&A, 468, 663 (Paper II)
- Takeda, Y., Ohkubo, M., & Sadakane, K. 2002, PASJ, 54, 451
- Takeda, Y., Ohkubo, M., Sato, B., Kambe, E., & Sadakane, K. 2005, PASJ, 57, 27
- Takeda, Y., Sato, B., & Murata, D. 2008, PASJ, 60, 781

Table 1. Target stars and their parameters

Star No.	HIP number	Name	Sp. type	$T_{\text{eff}}^{\text{std}}$ (K)	$\log g^{\text{std}}$ (cm s^{-1})	$v_{\text{t}}^{\text{std}}$ (km s^{-1})	$\{\text{Fe}/\text{H}\}^{\text{std}}$ (dex)	π (mas)	σ/π	$\log L$ (L_{\odot})	M (M_{\odot})	$\log age$ (yr)	$\langle v_{\text{rt}} \rangle$ (km s^{-1})	EW_{6708} (mÅ)	$A_{\text{Li}}^{\text{NLTE}}$
1	56948	...	G5	5747.9	4.409	0.93	-0.016	15.0	0.05	+0.13	0.98	9.90	2.18	3.6	1.13
2	79672	18 Sco	G1 V	5771.7	4.397	0.97	+0.011	71.3	0.01	+0.05	1.01	9.70	2.29	9.7	1.60
3	100963	...	G5	5760.0	4.411	0.93	-0.040	35.4	0.02	+0.02	1.00	9.66	2.27	12.1	1.68
0	...	Sun/Moon	G2 V	5737.1	4.420	0.95	-0.036	(0.00)	(1.00)	(9.66)	2.13	2.2	0.91

Notes:

In columns 5–8 are listed the $T_{\text{eff}}^{\text{std}}$ (effective temperature), $\log g^{\text{std}}$ (logarithmic surface gravity), $v_{\text{t}}^{\text{std}}$ (microturbulence), and $\{\text{Fe}/\text{H}\}^{\text{std}}$ ($\equiv A_{\text{Fe}}^{\text{std}} - 7.50$; metallicity), which are the “standard” atmospheric parameters spectroscopically determined based on the selected Fe I and Fe II lines (see subsection 3.1.1 of Paper II). Columns 9 and 10 present the Hipparcos parallaxes (ESA 1997) and their relative errors, while the values of luminosity, mass, and age are given in columns 11–13, which were derived from the positions on the theoretical HR diagram with the help of stellar evolutionary tracks (see subsection 3.3 of Paper II). The $\langle v_{\text{rt}} \rangle$ (column 14) is the rotational broadening parameter (nearly equivalent to the projected rotational velocity $v_e \sin i$) determined from the widths of a number of Fe I and Fe II lines (cf. subsection 3.2). The equivalent width of the Li I 6707.8 doublet and the logarithmic abundance of Li (including the relevant non-LTE correction of +0.07 dex for all four stars) in the usual normalization of $A_{\text{H}} = 12$ are presented in the last columns 15–16.

Table 2. Differential analysis of HIP 56948 relative to the Sun.

	[direct analysis]													
	ΔT	$\Delta \log g$	Δv_t	ΔA	ϵ_T	ϵ_g	ϵ_v	ϵ_{A_1}	ϵ_{A_2}	σ_{A_1}	σ_{A_2}	N_1	N_2	
056948 – Sun	+4.3	-0.015	-0.02	+0.015	5.0	0.010	0.04	0.007	0.008	0.021	0.021	196	18	
–(Sun – 056948)	+1.3	-0.027	-0.01	+0.012	5.0	0.010	0.04	0.006	0.007	0.020	0.018	189	16	
$\langle 056948 - \text{Sun} \rangle$	+2.8	-0.021	-0.01	+0.013										
	[indirect analysis]													
	ΔT	$\Delta \log g$	Δv_t	ΔA	σ_T	σ_g	σ_v	σ_A						
$\langle\langle 056948 - \text{Sun} \rangle\rangle$	+17.0	+0.006	-0.01	+0.020	3.8	0.012	0.01	0.004						
(via 079672)	+20.7	+0.018	-0.01	+0.024										
(via 100963)	+13.2	-0.006	+0.00	+0.016										
	[differences of standard parameters]													
	$\Delta T = 5747.9 - 5737.1 = +10.8$													
	$\Delta \log g = 4.409 - 4.420 = -0.011$													
	$\Delta v_t = 0.93 - 0.95 = -0.02$													
	$\Delta A = -0.016 - (-0.036) = +0.020$													

Notes.

The results of differential analyses for the case of ($i = 1$ and $j = 0$). The brief description of the data in the table is given below while Paper I should be consulted for more detailed explanations. (Note that the effective temperature T_{eff} and the Fe abundance A_{Fe} are abbreviated as T as A , respectively, in this table 2 along with the following tables 3 and 4.)

(Direct analysis:)

— 1st row: the results of (ΔT_{i-j} , $\Delta \log g_{i-j}$, Δv_{i-j} , ΔA_{i-j}), the possible errors (ϵ_T , ϵ_g , and ϵ_v) involved in these solutions (estimated by the procedure described in subsection 5.2 of Takeda et al. 2002), the root-mean-square errors (ϵ_{A_1} , ϵ_{A_2}) on the differential abundances ($\Delta A_{1,i-j}$ and $\Delta A_{2,i-j}$) from Fe I and Fe II lines corresponding to these ambiguities in atmospheric parameters, the standard deviations (σ_{A_1} and σ_{A_2}) around the means of $\Delta A_{1,i-j}$ and $\Delta A_{2,i-j}$, and the numbers (N_1 and N_2) of the used Fe I and Fe II lines.

— 2nd row: the same as the 1st row, but for the inverse case of $j - i$; i.e., presented are the parameter differences of ($-\Delta T_{j-i}$, $-\Delta \log g_{j-i}$, $-\Delta v_{j-i}$, and $-\Delta A_{j-i}$) and the corresponding errors (ϵ_T , ϵ_g , ϵ_v , ϵ_{A_1} , and ϵ_{A_2}).

— 3rd row: averaged solutions of the parameter differences given in the 1st and 2nd rows; i.e., $\langle \Delta T_{ij} \rangle$, $\langle \Delta \log g_{ij} \rangle$, $\langle \Delta v_{ij} \rangle$, and $\langle \Delta A_{ij} \rangle$.

(Indirect analysis:)

— The first row gives $\langle\langle \Delta p_{i(j)} \rangle\rangle$ [equation (15) in Paper I] and $\langle\langle \sigma_{\Delta p, i(j)} \rangle\rangle$ [equation (16) in Paper I], where p denotes each of T , $\log g$, v , and A .

— Meanwhile, in the following two rows are presented the individual $\langle \Delta p_{i(k)j} \rangle$ values [equation (14) in Paper I] for each intermediary star k (from which the $\langle\langle \Delta p_{i(j)} \rangle\rangle$ and $\langle\langle \sigma_{\Delta p, i(j)} \rangle\rangle$ values in the first row were computed).

(Inset in the lower-right space:)

— The ($i - j$) differences of the standard parameters (T , $\log g$, v , and A) given in table 1 .

Table 3. Differential analysis of HIP 79672 relative to the Sun.*

	[direct analysis]													
	ΔT	$\Delta \log g$	Δv_t	ΔA	ϵ_T	ϵ_g	ϵ_v	ϵ_{A_1}	ϵ_{A_2}	σ_{A_1}	σ_{A_2}	N_1	N_2	
079672 – Sun	+48.9	+0.008	+0.03	+0.056	5.0	0.010	0.03	0.006	0.006	0.018	0.016	194	17	
–(Sun – 079672)	+48.1	+0.009	+0.03	+0.053	5.0	0.010	0.03	0.006	0.006	0.019	0.017	193	17	
$\langle 079672 - \text{Sun} \rangle$	+48.5	+0.008	+0.03	+0.054										
	[indirect analysis]													
	ΔT	$\Delta \log g$	Δv_t	ΔA	σ_T	σ_g	σ_v	σ_A						
$\langle\langle 079672 - \text{Sun} \rangle\rangle$	+39.3	-0.013	+0.04	+0.048	8.8	0.018	0.00	0.004						
(via 056948)	+30.6	-0.031	+0.03	+0.044										
(via 100963)	+48.1	+0.005	+0.04	+0.052										
	[differences of standard parameters]													
	$\Delta T = 5771.7 - 5737.1 = +34.6$													
	$\Delta \log g = 4.397 - 4.420 = -0.023$													
	$\Delta v_t = 0.97 - 0.95 = +0.02$													
	$\Delta A = 0.011 - (-0.036) = +0.047$													

*The results of differential analyses for the case of ($i = 2$ and $j = 0$). See the notes in table 2 for the details.

Table 4. Differential analysis of HIP 100963 relative to the Sun.*

														[direct analysis]			
	ΔT	$\Delta \log g$	Δv_t	ΔA	ϵ_T	ϵ_g	ϵ_v	ϵ_{A_1}	ϵ_{A_2}	σ_{A_1}	σ_{A_2}	N_1	N_2				
100963 – Sun	+37.8	+0.021	+0.01	+0.003	0.0	0.010	0.04	0.005	0.007	0.019	0.013	194	18				
–(Sun – 100963)	+38.6	+0.026	–0.01	+0.005	0.0	0.010	0.03	0.005	0.006	0.018	0.014	188	17				
$\langle 100963 - \text{Sun} \rangle$	+38.2	+0.023	+0.00	+0.004													
														[indirect analysis]			
	ΔT	$\Delta \log g$	Δv_t	ΔA	σ_T	σ_g	σ_v	σ_A									
$\langle \langle 100963 - \text{Sun} \rangle \rangle$	+33.2	+0.018	–0.01	+0.004	5.4	0.009	0.00	0.002									
(via 056948)	+27.8	+0.009	–0.01	+0.001													
(via 079672)	+38.6	+0.027	–0.01	+0.006													
														[differences of standard parameters]			
														$\Delta T = 5760.0 - 5737.1 = +22.9$			
														$\Delta \log g = 4.411 - 4.420 = -0.009$			
														$\Delta v_t = 0.93 - 0.95 = -0.02$			
														$\Delta A = -0.040 - (-0.036) = -0.004$			

*The results of differential analyses for the case of ($i = 3$ and $j = 0$). See the notes in table 2 for the details.

Table 5. Summary of differential parameters relative to the Sun

Star	ΔT_{eff} (K)	$\Delta \log g$ (dex)	Δv_t (km s ^{–1})	ΔA_{Fe} (dex)	ΔA_{Li} (dex)	$\langle v_{\text{rt}} \rangle / \langle v_{\text{rt}}^{\odot} \rangle$
HIP 56948	+2.8	–0.021	–0.01	+0.013	+0.22	1.02
	+17.0	+0.006	–0.01	+0.020		
HIP 79672	+48.5	+0.008	+0.03	+0.054	+0.69	1.08
	+39.3	–0.013	+0.04	+0.048		
HIP 100963	+38.2	+0.023	+0.00	+0.004	+0.77	1.07
	+33.2	+0.018	–0.01	+0.004		

Notes:

Columns 2 through 5 present the “star–Sun” differences for each of the parameters (T_{eff} , $\log g$, v_t , and A_{Fe} ; final averaged results extracted from tables 2–4) resulting from the differential analysis based on the method of Paper I, where the values in the upper and lower row correspond to the direct solution ($\langle \langle \Delta p_{i0} \rangle \rangle$; cf. section 3 in Paper I) and the solution obtained via intermediary stars ($\langle \langle \Delta p_{i(0)} \rangle \rangle$; cf. section 4 in Paper I), respectively. Given in columns 6 and 7 are the differential Li abundance relative to the Sun and the “star/Sun” ratio of $\langle v_{\text{rt}} \rangle$ (rotational broadening parameter), respectively, which were simply obtained from the data in table 1.